SORCE SOLSTICE Release Notes for Version 18, Level 3 data products

J.P. Elliott, M. Snow, B. Vanier, E. Lieb, S. Mueller, W. Carande
Laboratory for Atmospheric and Space Physics, University of Colorado

SOLSTICE data Version 18 (V18) appears in three locations:

1. On the LISIRD website: http://lasp.colorado.edu/lisird/sorce/)
2. On the SORCE website: http://lasp.colorado.edu/home/sorce/data/
3. On the NASA DAAC:

FUV: https://disc.gsfc.nasa.gov/datasets/SOR3SOLFUVD_018/summary
MUV: https://disc.gsfc.nasa.gov/datasets/SOR3SOLMUVD_018/summary

Table 1 below gives a description of available time and wavelength ranges for each location.

An IDL reader for the ASCII formatted data present on the SORCE website is available at:
http://lasp.colorado.edu/data/sorce/file_readers/read_lasp_ascii_file.pro

Time Range	Wavelength Range (nm)	
04/14/2003 - 02/25/2020	115 - 180	180 - 310
	FUV	MUV

Table 1: Time and wavelength ranges for each repository location.

Calibration Changes

I. Splint correction

There is a systematic offset in the SOLSTICE data after the vacation period. For V18, we correct this offset with the “splint” correction. It is the result of taking the ratio between the NRL SSI model and SOLSTICE before and after the vacation period (roughly mission day 3500 to 4000). The previous spike correction (from v16) has been multiplied out of the SOLSTICE data and both sets of data, NRL and SOLSTICE, were averaged over 10 days before the ratio was taken. The correction is the result of the ratio of the ratios before and after the vacation of NRL and SOLSTICE:

$$corr = \frac{\left(\frac{SOL_{before}}{NRL_{before}}\right)}{\left(\frac{SOL_{after}}{NRL_{after}}\right)}$$

The following plot is the result of applying this correction.

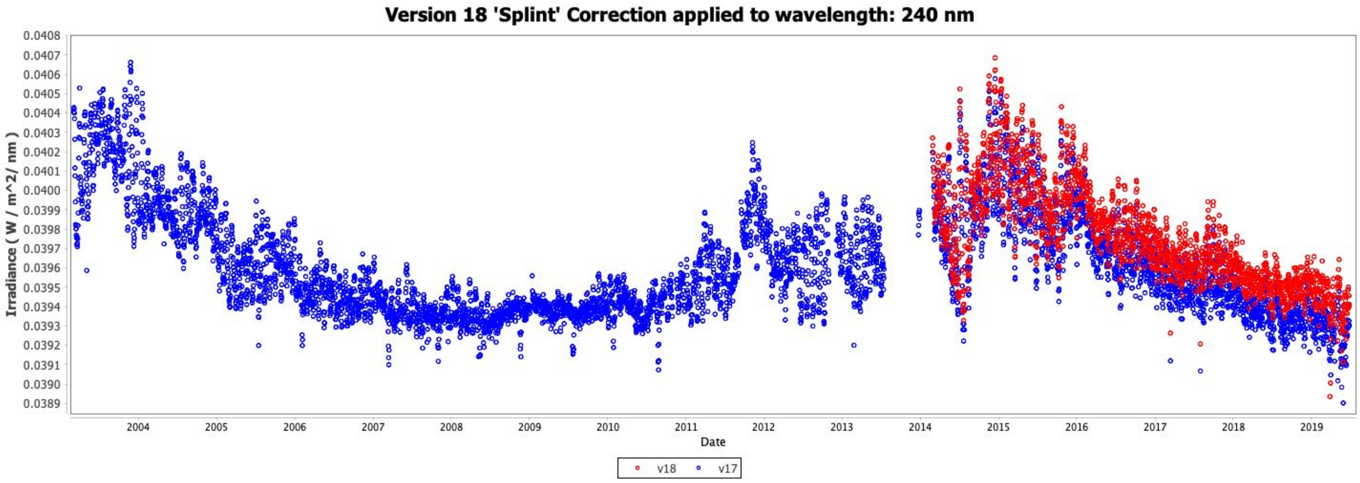

II. Spiders correction

In 2018, the SOLSTICE team discovered systematic anomalies in the SOLSTICE data at times corresponding to FOV map scans. Using the NRL SSI model, this correction was derived by taking the total average of NRL and SOLSTICE for 13 days before a given “spider”, taking the ratio of those averages and then dividing that ratio by the ratio of the SOLSTICE irradiance over the NRL irradiance for each day inside a “spider”. The correction factor, therefore, is defined as:

$$corr = \frac{\left(\frac{SOL_{before}}{NRL_{before}}\right)}{\left(\frac{SOL_{after}}{NRL_{after}}\right)}$$

This correction factor is then multiplied by the SOLSTICE spider irradiance for each day inside each spider to bring the value of the "spiders" up. The following plot is the result of this application to one spider.

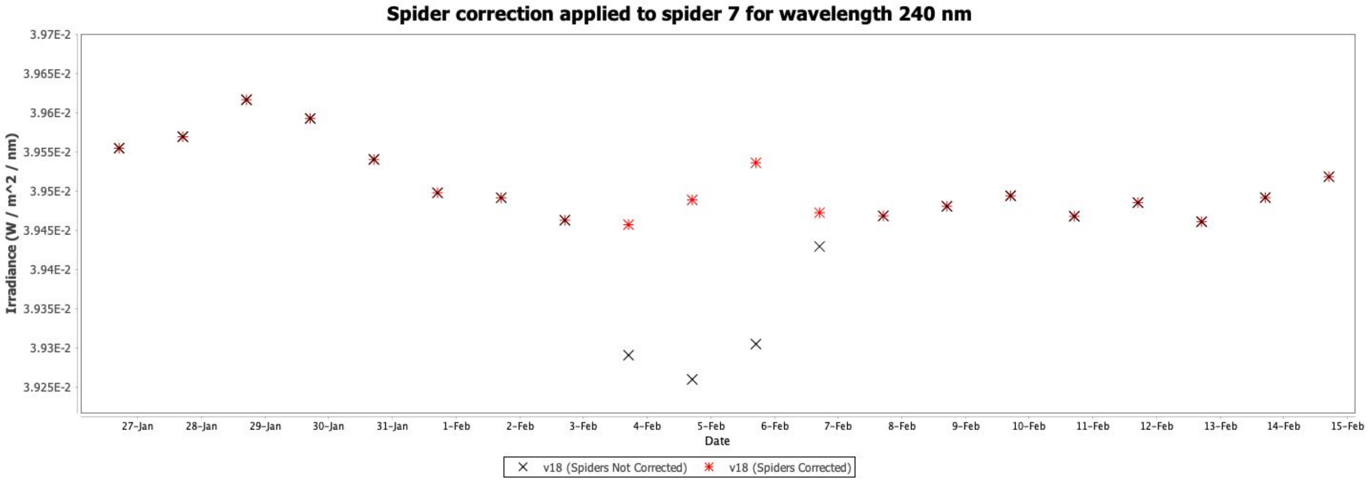

III. Stable/Up/down/integration time correction

Systematic offsets occur for different instrument scan modes. During a normal scan across the spectrum, the reflection grating rotates over the spectrum and then reverses direction to collect the spectrum again, doubling the number of samples across the full wavelength range. The first portion of the scan consistently yields a systematically higher count rate than the second portion of the scan. Other types of scanning activities also yielded different systematic offsets.

Two main factors contributed to these offsets. The first was determined to be slight changes in the stability of the measurement due to the mechanical motions of some of the optical elements in the instrument, such as filter motion, ellipse mirror motion as well as scan direction (as mentioned above). The second had to do with slight changes in the true integration time of each measurement as opposed to the reported integration time. This was measured towards the end of spacecraft operations by a set of integration time tests which revealed the problem.

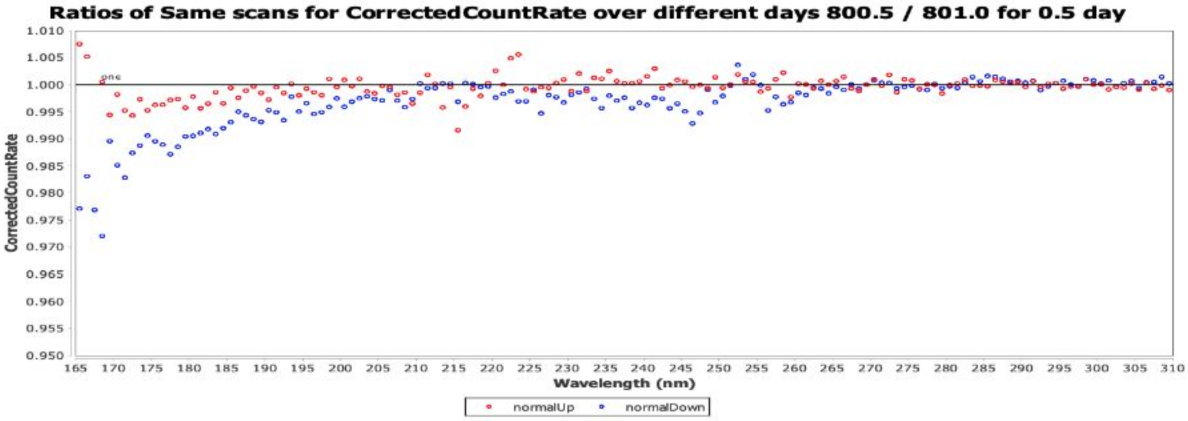

The final correction is based off of ellipse stability, integration time, scan direction, wavelength, and time. This correction is usually less than 1%. All scans are normalized to normal up experiments.

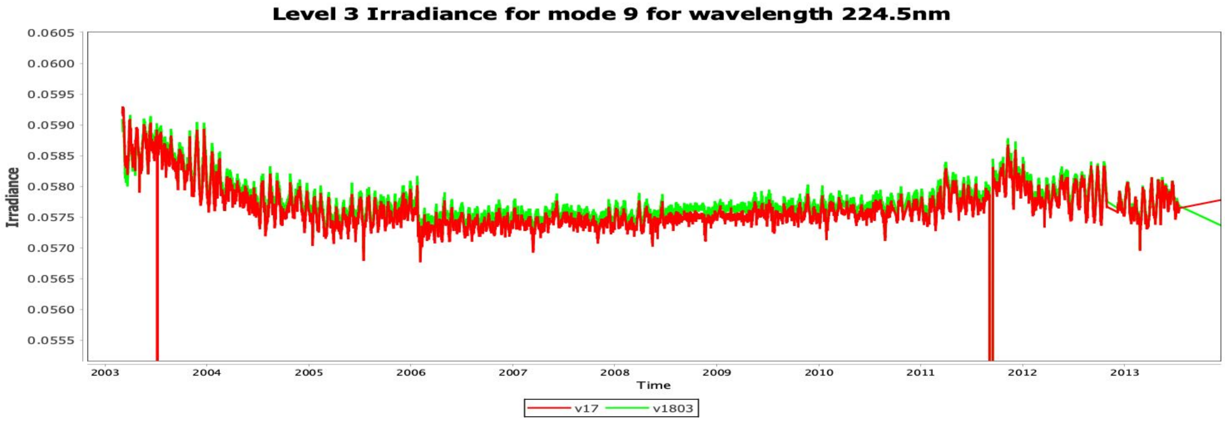

IV. Temperature Correction

An updated temperature correction has been included with V18 in order to better account for temperature fluctuations, especially in the latter part of the mission when the spacecraft had poor temperature control due to necessary power cycling on every orbit.

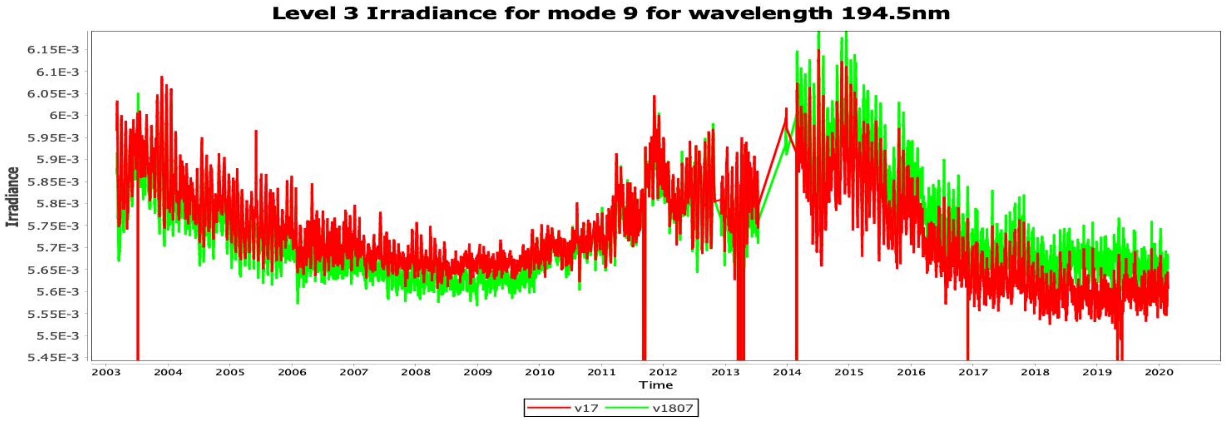

V. AB Calibration

An updated cross calibration between the MUV channels of SOLSTICE A and SOLSTICE B was performed. Previously this was calculated on a 1nm binned grid. Our new correction uses a 0.25nm grid in order to capture higher resolution spectral structure. The correction is also time dependent and so changes throughout the mission.

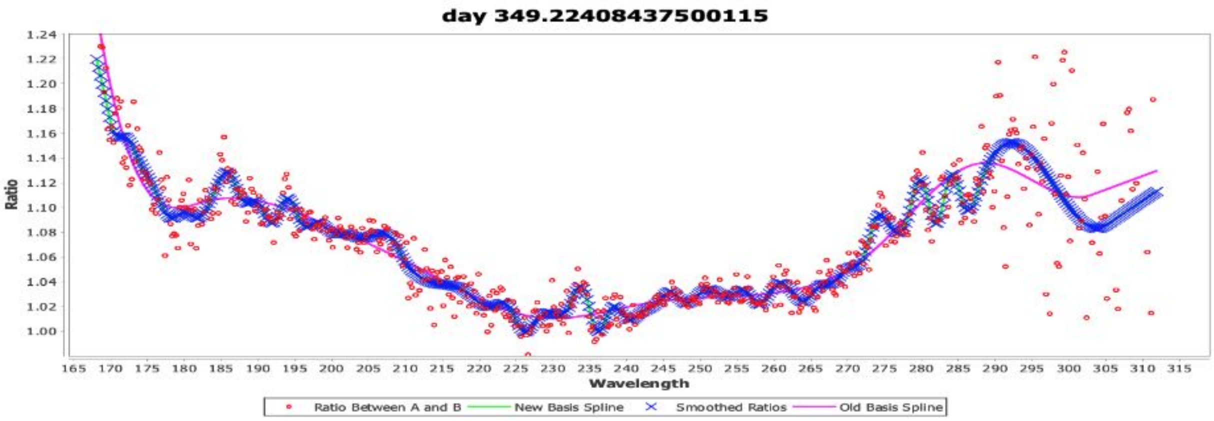

VI. Lyman-Alpha Geocoronal Correction

The Earth's Hydrogen exosphere scatters light near the Lyman-Alpha wavelength at 121.6nm. The SORCE spacecraft orbits within this exosphere resulting in an attenuation of signal at the Lyman-Alpha spectral feature. The attenuation varies as a function of orbital position. Or, more specifically, the attenuation is proportional to the Solar Zenith Angle (SZA), which is the angle between the Sun-spacecraft vector and a vector pointing from the spacecraft radially away from the Earth. At high SZA the spacecraft observes the Sun through a much longer column of exospheric Hydrogen as compared to low SZA.

We calculate a correction to this attenuation. The geocoronal correction fit coefficients are calculated separately for dawn and dusk data. An additional filter is applied to ensure normalized irradiance values are between 0.98 and 1.02. The "y" value is normalized irradiance, the "x" value is the average solar zenith angle (SZA). The input/output values for the script are as follows:

- Input: start and stop dates, frequency of fit (daily, monthly, yearly, all points), type of fit (polynomial, cosine)
- Output: equation coefficients, r_squared (size of these depends on whether you specify daily/monthly/yearly/all)

  For each year, we have coefficients a and b, where:

$$y = a \cos(b\, x)$$

Note: The b coefficient includes the conversion factor from degrees to radians. x is in degrees.

Before fitting a curve to the data, there are several pre-processing and filtering steps. Miniscan start and stop times are retrieved from the planning and scheduling database. For each miniscan time range, we query the wavelength and irradiance tables, query the target view parameters table for target zenith angle, and interpolate target zenith angle to match the times of the wavelength/irradiance measurements (using linear interpolation). Forward/backward times are defined using and shift in solar zenith angle (SZA) where forward indicates declining SZA and backward indicates increasing SZA. We find boundary points where there are changes in the sign of the wavelength shift. Next, we find steps between each boundary point, excluding the points at the beginning and end of miniscan and any periods where the number of points between boundary points is less than 64. For each step within the miniscan, we apply a Lyman-alpha filter so the wavelength is between 121.3nm and 121.8nm, take the sum of irradiance with Lyman-alpha filter applied, find the average SZA and average GPS microseconds: mean of GPS microsecond timestamps. Dawn and dusk times are defined by positive (dusk) or negative (dawn) shifts in the average SZA. Finally, we normalize the irradiance around a SZA of 60 degrees.

The procedure is valid for the 2003 to 2012 time range because after 2012 the instrument activities changed and prevented us from being able to fit the data properly. For each year 2003 to 2012, the cosine function is fit to the normalized irradiance vs. average zenith angle curve with a different fit for dusk and dawn times. The plot below shows the dawn fits for all years.

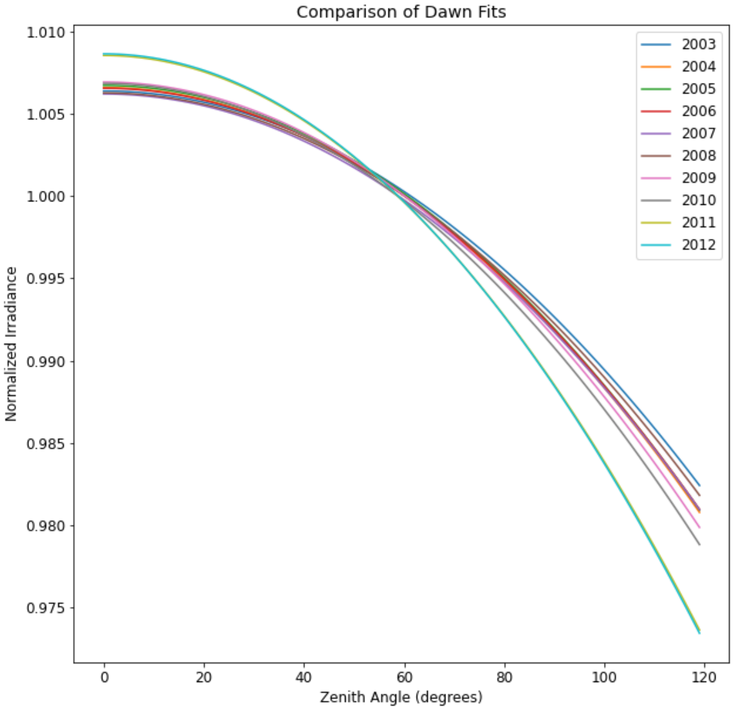

For 2003 to 2012 we use the yearly computed correction coefficients, as seen in the plot below.

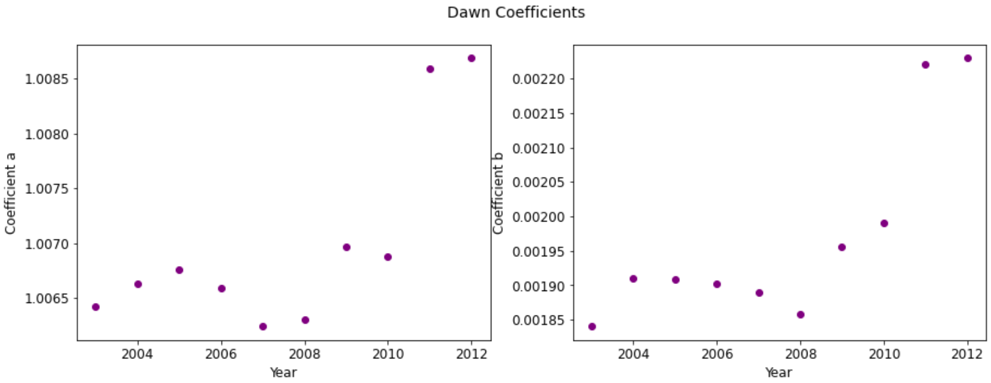

For the dawn coefficients, please note that 2011 and 2012 are outliers. This is an effect that needs further evaluation and study. For 2013 and 2014, we use the average of the 2011 and 2012 coefficients. For 2015 to present, we use the average of the 2003 to 2010 coefficients. These average coefficients are plotted as orange and blue lines in the plot below.

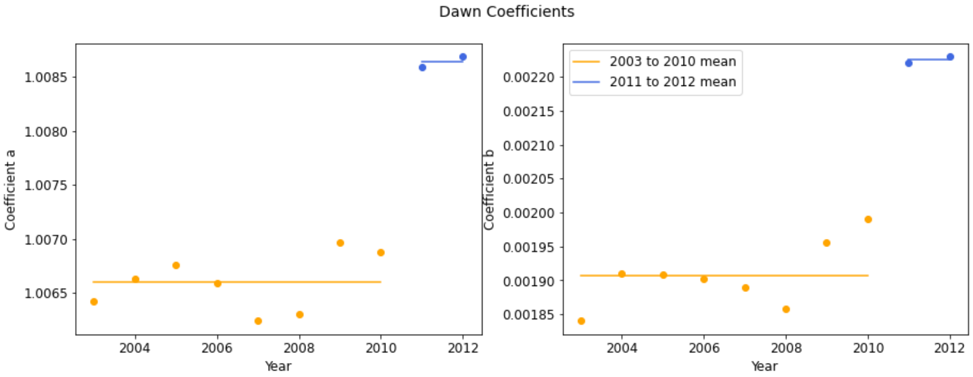

Similar to the dawn fits, the plot below shows the dusk fits for all years.

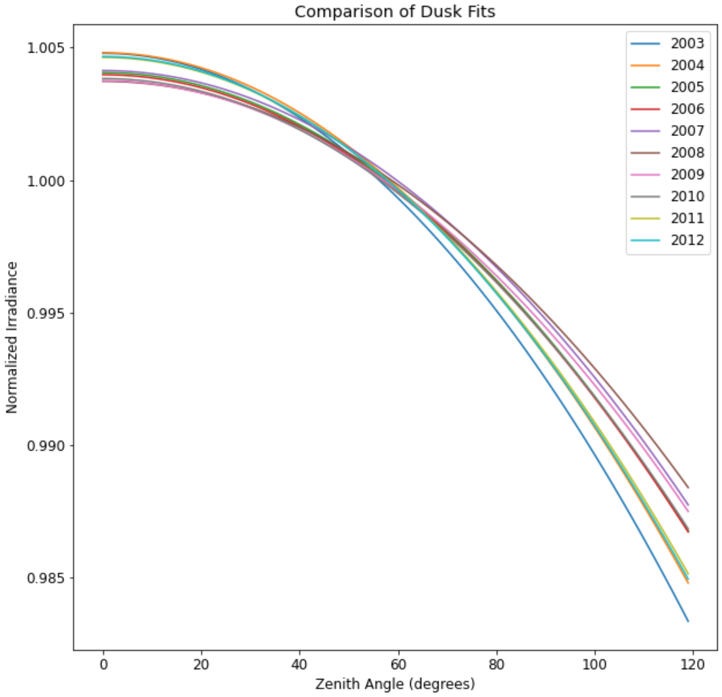

For 2003 to 2012 we use the yearly computed correction coefficients, as seen in the plot below.

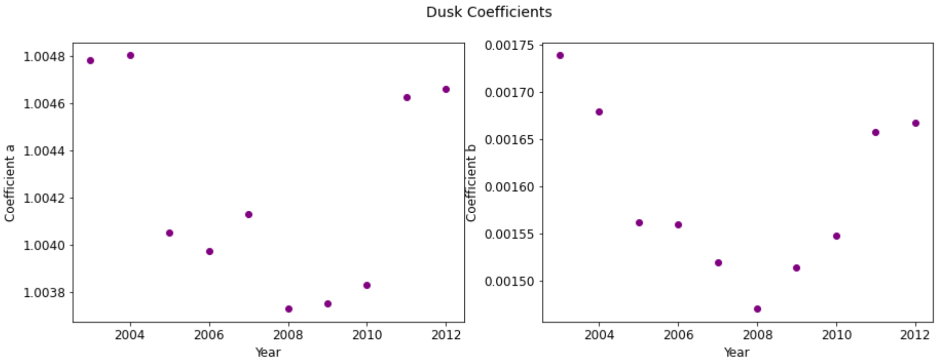

Note that there appears to be a cyclic pattern in the dusk coefficients. For 2013 to present we use the average of the 2004 to 2009 coefficients. This average is represented by the line in the plot below.

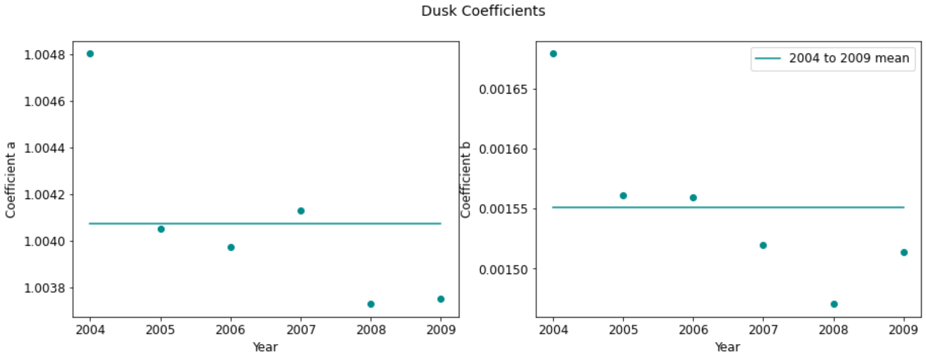

The resulting corrected irradiance is plotted below.

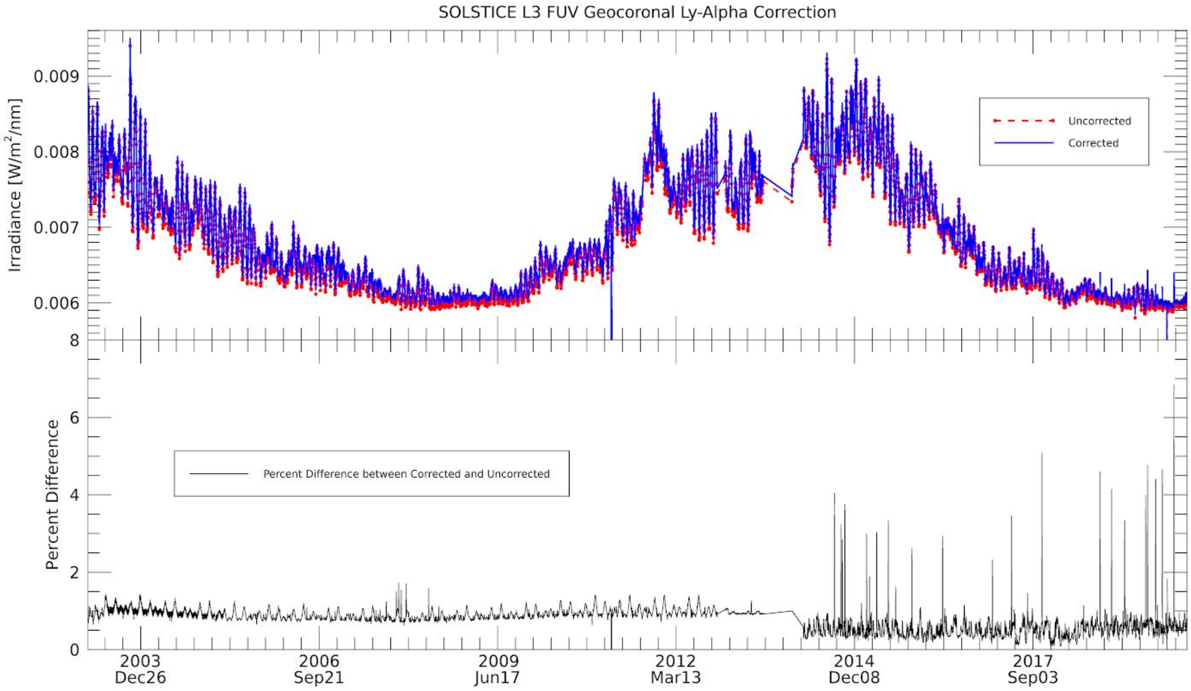

Algorithm Changes

I. Magnesium II Index

We have updated our Magnesium II index algorithm to match Snow et al. 2019.

The MgII Index, also referred to as the MgII core-to-wing ratio, is a proxy for chromosphere activity. Dating from the late 1970's, the MgII Index represents one of the longest records of solar variability.

The chromospheric MgII h and k lines, located at 280.27 nm and 279.56 nm, respectively, represent the numerator of the MgII ratio. These MgII "cores" are divided by the highly stable (at least on short timescales) photospheric "wing" contributions. The wings are broadband irradiance ranges located on either side of the cores. The blue wing consists of irradiances from 275.83 nm to 279.00 nm, and the red wing consists of irradiances from 280.83 nm to 284.0 nm.

Two MgII Index products are generated – a daily (Level 3) product and a per-scan (Level 2) product. There are 5828 L3 MgII Index values, one for each viable mission day. Because there are multiple scans per day, there are well over 100,000 L2 MgII Index values. These values are ingested into the database and preserved as IDL ***.sav*** files. Uncertainties are also determined.

Irradiances are mapped onto a regular 0.02 nm grid using a cubic spline interpolation. A set of scaling factors, which consist of an offset and a multiplicative factor, may be applied to the result.

Below is the v18 L2 MgII Index

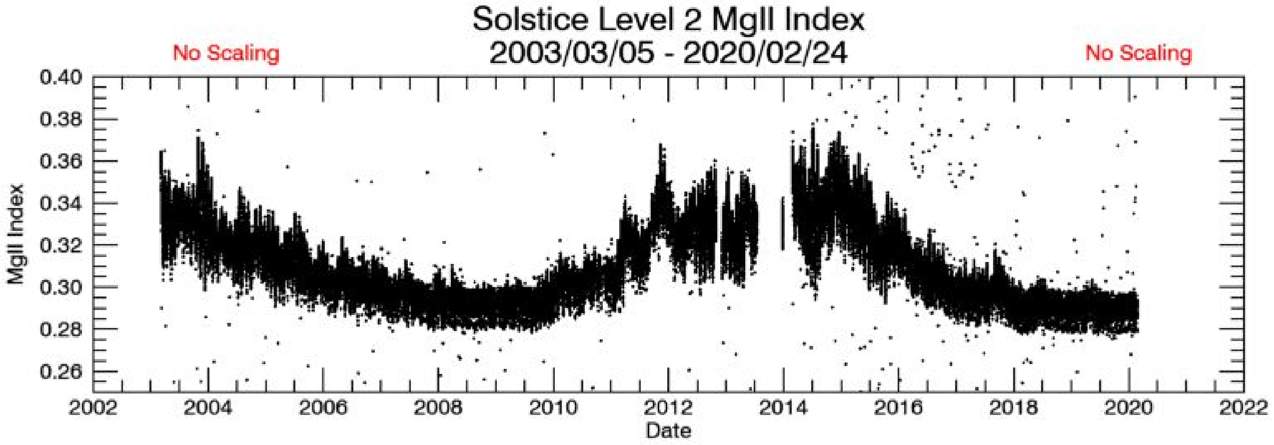

Weights

The MgII Index is a weighted ratio, in which the measured irradiances are multiplied by a wavelength-dependent weight and the sum of the weighted values is normalized by the sum of the weights. The core weights are modeled as simple step functions (0 or 1 everywhere), whereas the wing weights are modeled as trapezoids.

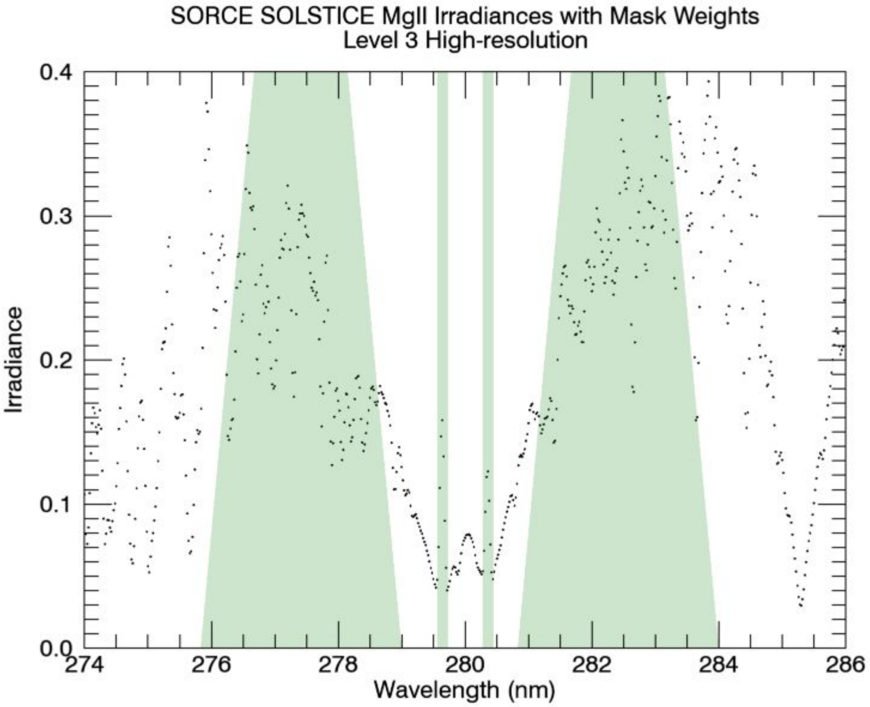

The blue wing weighting trapezoid is defined as
$bw_1 = 275.83$; left base of trapezoid
$bw_2 = 276.67$; left peak of trapezoid
$bw_3 = 278.15$; right peak of trapezoid
$bw_4 = 279.00$; right base of trapezoid

and the corresponding weighting function is
$w = 0$ for $\lambda < bw_1$
$w = (\lambda - bw_1)/(bw_2 - bw_1)$ for $bw_1 \leq \lambda < bw_2$
$w = 1$ for $bw_2 \leq \lambda \leq bw_3$
$w = (\lambda - bw_4)/(bw_3 - bw_4)$ for $bw_3 < \lambda \leq bw_2$
$w = 0$ for $\lambda > bw_4$

The red wing weighting trapezoid is defined as
$rw_1 = 280.83$; left base of trapezoid
$rw_2 = 281.67$; left peak of trapezoid
$rw_3 = 283.15$; right peak of trapezoid
$rw_4 = 284.00$; right base of trapezoid

and the corresponding weighting function is
$w = 0$ for $\lambda < rw_1$
$w = (\lambda - rw_1)/(rw_2 - rw_1)$ for $rw_1 \leq \lambda < rw_2$
$w = 1$ for $rw_2 \leq \lambda \leq rw_3$
$w = (\lambda - rw_4)/(rw_3 - rw_4)$ for $rw_3 < \lambda \leq rw_2$
$w = 0$ for $\lambda > rw_4$

MgII Index

The weighted ratio is of the form

$$MgII\ Index = \frac{\frac{\Sigma(i_{h,n})}{\Sigma(w_{h,n})} + \frac{\Sigma(i_{k,n})}{\Sigma(w_{k,n})}}{\frac{\Sigma(w_{bw,n} * i_{bw,n})}{\Sigma(w_{bw,n})} + \frac{\Sigma(w_{rw,n} * i_{rw,n})}{\Sigma(w_{rw,n})}}$$

in which i_h represents the h-line irradiances, i_k represents the k-line irradiances, i_{bw} represented the blue wing irradiances, i_{rw} represents the red wing irradiances, w_h represents the h-line weights, w_k represents the k-line weights, w_{bw} represents the blue wing weights, and w_{rw} represents the red wing weights.

Uncertainties

The individual measurement uncertainties are

$$\delta h = h\text{–}line\ Error = \sqrt{\Sigma(\Delta i_{h,n})^2}$$

$$\delta k = k\text{–}line\ Error = \sqrt{\Sigma(\Delta i_{k,n})^2}$$

$$\delta bw = Blue\ Wing\ Error = \sqrt{\Sigma(\Delta i_{bw,n})^2}$$

$$\delta rw = Red\ Wing\ Error = \sqrt{\Sigma(\Delta i_{rw,n})^2}$$

In which Δ represents the uncertainty associated with an individual measurement. It follows that the uncertainty in the MgII ratio is

$$\delta \text{MgII} = \text{MgII}\sqrt{(\frac{\delta h}{h})^2 + (\frac{\delta k}{k})^2 + (\frac{\delta bw}{bw})^2 + (\frac{\delta rw}{rw})^2}$$

New Data Products

I. Lyman-Alpha High Cadence Scan Product

For V18 we have released for the first time high-cadence Lyman-Alpha scans at full spectral and temporal resolution. Up until 2012 these scans were performed but were not released as a separate product until now. After 2012 due to changes in spacecraft and instrument operations these scans were no longer possible and therefore are only available prior to that.

Each day can contain multiple scans which look like the following plot.